HAL
open science

A Self-Reconfigurable and Fault-Tolerant Induction Motor Control Architecture for Hybrid Electric Vehicles

Mickaël Hilairet, Demba Diallo, Mohamed Benbouzid

To cite this version:

Mickaël Hilairet, Demba Diallo, Mohamed Benbouzid. A Self-Reconfigurable and Fault-Tolerant Induction Motor Control Architecture for Hybrid Electric Vehicles. ICEM'06, Sep 2006, Chania, Greece. 6pp. hal-00527572

HAL Id: hal-00527572

https://hal.science/hal-00527572v1

Submitted on 19 Oct 2010

HAL is a multi-disciplinary open access archive for the deposit and dissemination of scientific research documents, whether they are published or not. The documents may come from teaching and research institutions in France or abroad, or from public or private research centers.

L'archive ouverte pluridisciplinaire **HAL**, est destinée au dépôt et à la diffusion de documents scientifiques de niveau recherche, publiés ou non, émanant des établissements d'enseignement et de recherche français ou étrangers, des laboratoires publics ou privés.

A self-reconfigurable and fault-tolerant induction motor control architecture for hybrid electric vehicles

M. Hilairet, D. Diallo and M.E.H. Benbouzid

***Abstract*— This paper describes an adaptive control system for an induction motor drive that propels a Hybrid Electrical Vehicle (HEV). It has been designed to comply with the major requirements of HEVs electric propulsion. The fault tolerant controller is based on a Field Oriented Control with 4 IP regulators, a speed sensor and two observers (Extended Kalman Filter (EKF) and an Adaptive Observer (AO)) to guarantee the best dynamic performances required by the application and also to improve the reliability in the event of sensor loss or sensor recovery. The tuning of the observers is based on extensive simulations, experimental results and optimization procedure within an open-loop type approach. The fault tolerant controller reorganization is based on a control decision block implemented with a Maximum Likelihood voting algorithm. The results of the control system show the effectiveness of the approach. Indeed experimental results of the EKF used in closed loop confirm the validity of the sensorless controller and the fault tolerant controller simulation results in the event of speed sensor loss and recovery are very promising even in case of stator resistance variation.**

***Index Terms*— Fault tolerant, induction motor drive, hybrid electric vehicule, observers.**

I. Introduction

Cage induction motors are widely accepted as the most potential candidate for the electric propulsion of HEVs according to their reliability, ruggedness, low maintenance, low cost, and ability to operate in hostile environments. They are particularly well suited for the rigors of industrial and traction drive environments. Today, induction motor drive is the most mature technology among various commutatorless motor drives. Moreover, the cage induction motor seems to be the candidate that better fulfils the major requirements of automotive electric traction [1].

Several failures afflict electrical motor drives [1] and so far, redundant or conservative design has been used in every application where continuity of operations is a key feature. This is the case of home and civil appliances, such as, for example, air conditioning/heat pumps, engine cooling fans, and electric vehicles. This is especially important in high impact automotive applications, such as EV and HEV, where even limp-back operation is preferred over no operation.

Fault-tolerance has become an increasingly interesting topic in the last decade where the automation has become more complex. A trend towards more autonomic control systems also drives the interest for fault-tolerance. In mass produced industrial systems the unit cost is a paramount issue. Hence cheap fault-tolerant control has become an important industrial research area. The objective is to give solutions that provide fault-tolerance to the most frequent faults and thereby reduce the costs of handling the faults. The fault tolerant controller also increases the reliability of the process.

The study reported in this paper is concerned with the problem of developing an induction motor drive with tolerance to the speed sensor failure. This paper describes an active fault-tolerant control system for a high performance induction motor drive that propels an Electrical Vehicle (EV) or a Hybrid one (HEV). The proposed system adaptively reorganizes itself in the event of sensor loss or sensor recovery to sustain the best control performance given the complement of remaining sensors. The control reorganization is managed by a voting algorithm system that assures smooth transition from the nominal controller to the sensorless one and back to the encoder-based controller. Simulations tests using collected experimental data, in term of speed and torque responses, have been carried out on a 1.2kW induction motor to evaluate the consistency and the performance of the proposed fault-tolerant control approach.

In the next paragraph, the encoder-based nominal controller is briefly described and the sensorless controller using an Extended Kalman Filter (EKF) and an Adaptive Observer (AO) is presented within the fault-tolerant strategy. In the third part, the tuning and the validation of the observers based on the experimental benchmark data are introduced. In the fourth part the voting algorithm reliability coefficients computation is presented and the fault-tolerant controller tests are performed to show the validity of the approach.

II. Control philosophy

A. Nominal controller

The proposed control system has been designed to comply with the major requirements of HEVs electric propulsion: High torque at low speeds for starting and

Manuscript received June 30, 2006.

M. Hilairet and D. Diallo are with the Laboratoire de Génie Electrique de Paris LGEP/SpeeLabs, CNRS UMR 8705, Supelec, Universités Paris VI et XI, 11 rue Joliot Curie, F-91192 Gif sur Yvette cedex, France, E-mail: {mickael.hilairet,demba.diallo}@lgep.supelec.fr.

M.E.H. Benbourid is with the Laboratoire d'Ingénierie Mécanique et Electrique (LIME), IUT of Brest, University of Western Brittany - Rue de Kergoat, BP 93169, 29231 Brest Cedex 3, France, E-mail: m.benbouzid@ieee.org.

climbing, as well as high power at high speed for cruising; Very wide speed range including constant-torque and constant-power regions; Fast torque response; High efficiency over wide speed and torque ranges (Fig. 1). Indeed, the control system adaptively reorganizes itself according to the HEV tractive effort. The control system reorganization is based either on the accommodation of the actual control technique [2] or on the choice of a new one more adapted to the electric propulsion operation conditions [3], [4].

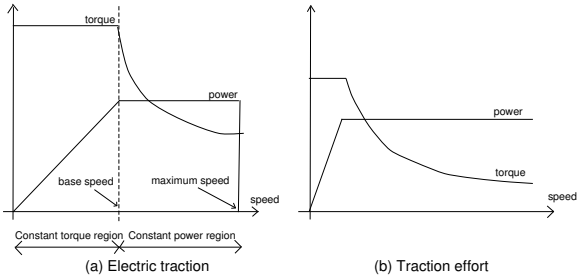

Fig. 1. HEV typical characteristics.

Depending upon the application and availability of sensors, and the desired performance of the system, there are many hybrid schemes that could be combined for fault-tolerant purposes. To satisfy the stringent requirements placed on high performance EV or HEV, induction motor vector control is a good candidate which has already proved its efficiency with a quick and precise torque for example. Therefore a nominal encoder-based controller using Indirect Field Orientation is used as the main controller. To maintain a good level of performance in vector control a speed estimator is mandatory to evaluate accurately the rotating reference frame position. The speed estimation is abundantly treated in the literature using advanced signal processing technique and linear or non linear automatic control theories. The first ones suffer from weak speed tracking error during transient and is prone to instability [5]. Among the second ones some methods are widely used like the extended Luenberger observers [6], [7], the Extended Kalman Filter (EKF) [7]–[10] or Adaptive Observers (AO) [11]–[17]. In this application the EKF and the AO are used for the sensorless controller. The self-reconfigurable and fault-tolerant controller comprises the nominal controller and the control decision block based on a voting algorithm for the choice of the fallback strategy.

B. Speed sensorless control

1) Motor model: The usual model of an induction motor is described by a fourth order state space model, with the stator voltages as inputs, the stator currents as measured outputs and the components of stator current and rotor flux as internal states. In the (α, β) stator reference frame, this state space model is :

$$\left\{ \begin{array}{rcl} \frac{d}{dt} X(t) & = & A_c(\omega_m)\, X(t) + B_c\, U(t) \\ Y(t) & = & C\, X(t) \end{array} \right.$$

$$\begin{array}{rcl} U & = & \left[\begin{array}{cc} V_{s\alpha} & V_{s\beta} \end{array} \right]^t \qquad Y = \left[\begin{array}{cc} i_{s\alpha} & i_{s\beta} \end{array} \right]^t \\ X & = & \left[\begin{array}{cccc} i_{s\alpha} & i_{s\beta} & \Phi_{r\alpha} & \Phi_{r\beta} \end{array} \right]^t \\ B_c & = & \left[\begin{array}{cccc} a & 0 & 0 & 0 \\ 0 & a & 0 & 0 \end{array} \right]^t \quad C = \left[\begin{array}{cccc} 1 & 0 & 0 & 0 \\ 0 & 1 & 0 & 0 \end{array} \right] \\ A_c(\omega_m) & = & \left[\begin{array}{cccc} \alpha & 0 & \beta & c\,\omega_m \\ 0 & \alpha & -c\,\omega_m & \beta \\ \gamma & 0 & \delta & -\omega_m \\ 0 & \gamma & \omega_m & \delta \end{array} \right] \end{array}$$

$$\begin{array}{rclrcl} \alpha & = & -(a\,R_s + c\,M_{sr}/T_r) & \beta & = & c/T_r \\ \gamma & = & M_{sr}/T_r & \delta & = & -1/T_r \\ a & = & 1/(\sigma\,L_s) & c & = & (1-\sigma)/(\sigma\,M_{sr}) \\ \sigma & = & 1 - M_{sr}^2/(L_s\,L_r) & T_r & = & L_r/R_r \end{array}$$

where $\omega_m = p\,\Omega$, Ω is the rotor velocity and $2\,p$ is the number of poles. The induction machine parameters are given in the appendix.

2) Discrete-time modeling: For the implementation of a flux estimator on a microcontroller, a discrete-time state space model is required. Provided that the input vector U is nearly constant during a sampling period T_s ($T_s = 125\ \mu s$), the previous continuous-time model leads to the following discrete-time state space model [18] :

$$\left\{ \begin{array}{rcl} X[k+1] & = & A(\omega_m)\, X[k] + B\, U[k] \\ Y[k] & = & C\, X[k] \end{array} \right.$$

The evaluation of $A(\omega_m) = e^{A_c T_s}$ can be performed by means of Sylvester's theorem because the matrix A_c has two distinct complex eigenvalues. Mathematically, this leads to an exact discrete-time modeling of the induction motor, but parameter uncertainties (due to thermal variation and saturation) cause state space errors which are more important than the discretization effect. This reduces the interest of the exact computation [19].

Therefore, a second order series expansion of the matrix exponential is used :

$$\begin{array}{rcl} e^{A_c\,T_s} & \approx & A = I + A_c\,T_s + (A_c\,T_s)^2/2 \\ A_c^{-1}\,(e^{A_c\,T_s} - I)\,B_c & \approx & B = T_s\,(I + (A_c\,T_s)/2)\,B_c \end{array}$$

This leads to :

$$A(\omega_m) = \left[\begin{array}{cccc} a_{11} & b_{11} & a_{12} & b_{12} \\ -b_{11} & a_{11} & -b_{12} & a_{12} \\ a_{21} & b_{21} & a_{22} & b_{22} \\ -b_{21} & a_{21} & -b_{22} & a_{22} \end{array} \right]$$

$$B = \left[\begin{array}{cccc} a_1 & 0 & a_2 & 0 \\ 0 & a_1 & 0 & a_2 \end{array} \right]^t$$

$$\begin{array}{rrcl} \text{with} & a_{11} & = & 1 + \alpha\,T_s + (\alpha^2 + \beta\,\gamma)\,T_s^2/2 \\ & a_{12} & = & \beta\,T_s\,(1 + (\alpha+\delta)\,T_s/2) + c\,\omega_m^2\,T_s^2/2 \\ & a_{21} & = & \gamma\,T_s\,(1 + (\alpha+\delta)\,T_s/2) \\ & a_{22} & = & 1 + \delta\,T_s + (\delta^2 + \beta\,\gamma)\,T_s^2/2 - \omega_m^2\,T_s^2/2 \\ & b_{11} & = & c\,\gamma\,\omega_m\,T_s^2/2 = -c\,b_{21} \\ & b_{12} & = & (c\,T_s\,(1 + (\alpha+\delta)\,T_s/2) - \beta\,T_s^2/2)\,\omega_m \\ & b_{21} & = & -\gamma\,\omega_m\,T_s^2/2 \\ & b_{22} & = & (-T_s + (c\,\gamma - 2\,\delta)\,T_s^2/2)\,\omega_m \\ & a_1 & = & a\,T_s\,(1 + \alpha\,T_s/2), \quad a_2 = a\,\gamma\,T_s^2/2 \end{array}$$

TABLE I
CONVENTIONAL EXTENDED KALMAN FILTER EQUATIONS

State and parameters prediction
$X[k+1\|k] = A[k]\,X[k\|k] + B[k]\,U[k]$
$\Theta[k+1\|k] = \Theta[k\|k]$
A priori covariance matrix computation
$P[k+1\|k] = F[k]\,P[k\|k]\,F[k]^t + Q$
$F[k] = \begin{bmatrix} A[k] & \frac{\partial}{\partial\Theta}(A[k]\,X[k\|k] + B\,U[k])_{\Theta[k\|k]} \\ 0 & I \end{bmatrix}$
Kalman gain computation
$K[k+1] = P[k+1\|k]\,H^t(H\,P[k+1\|k]\,H^t + R)^{-1}$
$H = \begin{bmatrix} C & 0 \end{bmatrix}$
State and parameters correction
$\begin{bmatrix} X[k+1\|k+1] \\ \Theta[k+1\|k+1] \end{bmatrix} = \begin{bmatrix} X[k+1\|k] \\ \Theta[k+1\|k] \end{bmatrix} + K[k+1]\,(Y[k+1] - C\,X[k+1\|k])$
A posteriori covariance matrix computation
$P[k+1\|k+1] = P[k+1\|k] - K[k+1]\,H\,P[k+1\|k]$

3) Extended Kalman filter: The conventional equations of the EKF [20] are summarized in Table I. If the rotor velocity is assumed nearly constant between two time samples, $\Theta[k] = \omega_m[k] \approx \omega_m[k-1]$, the matrices $F[k]$ and H are :

$$F[k] = \begin{bmatrix} a_{11} & b_{11} & a_{12} & b_{12} & f_1 \\ -b_{11} & a_{11} & -b_{12} & a_{12} & f_2 \\ a_{21} & b_{21} & a_{22} & b_{22} & f_3 \\ -b_{21} & a_{21} & -b_{22} & a_{22} & f_4 \\ 0 & 0 & 0 & 0 & 1 \end{bmatrix}$$

$$H = \begin{bmatrix} 1 & 0 & 0 & 0 & 0 \\ 0 & 1 & 0 & 0 & 0 \end{bmatrix}$$

$$\begin{aligned} \text{with } f_1 &= 0.5\,c\,\gamma T_s^2\,i_{s\beta}[k|k] + c\,T_s^2\,\omega_m[k|k]\,\Phi_{r\alpha}[k|k] \\ &+ (c\,T_s\,(1+(\alpha+\delta)\,T_s/2) - \beta\,T_s^2/2)\,\Phi_{r\beta}[k|k] \\ f_2 &= -0.5\,c\,\gamma T_s^2\,i_{s\alpha}[k|k] + c\,T_s^2\,\omega_m[k|k]\,\Phi_{r\beta}[k|k] \\ &- (c\,T_s\,(1+(\alpha+\delta)\,T_s/2) - \beta\,T_s^2/2)\,\Phi_{r\alpha}[k|k] \\ f_3 &= -0.5\,\gamma\,T_s^2\,i_{s\beta}[k|k] - T_s^2\,\omega_m[k|k]\,\Phi_{r\alpha}[k|k] \\ &+ (0.5\,(c\,\gamma - 2\,\delta)\,T_s^2 - T_s)\,\Phi_{r\beta}[k|k] \\ f_4 &= 0.5\,\gamma\,T_s^2\,i_{s\alpha}[k|k] - T_s^2\,\omega_m[k|k]\,\Phi_{r\beta}[k|k] \\ &- (0.5\,(c\,\gamma - 2\,\delta)\,T_s^2 - T_s)\,\Phi_{r\alpha}[k|k] \end{aligned}$$

Obviously, this extended Kalman filter has a heavier computational cost with a rough implementation. The use of a two-stage extended Kalman filter reduces the computation time by 25% by reducing the number of operations [21].

The main parameters of a Kalman filter are the covariance matrices Q and R, which are bound respectively to the state and measurement noises. The Kalman gain is insensitive to both Q and R multiplication by a scalar. Moreover the components on the α and β axes can be considered as statistically orthogonal and as there is no reason to consider differently the elements of the two pairs $(i_{s\alpha}, i_{s\beta})$ and $(\Phi_{r\alpha}, \Phi_{r\beta})$, we restrict ourselves to only three degrees of freedom :

$$R = \begin{bmatrix} 1 & 0 \\ 0 & 1 \end{bmatrix}, Q = \begin{bmatrix} \alpha_1 & 0 & 0 & 0 & 0 \\ 0 & \alpha_1 & 0 & 0 & 0 \\ 0 & 0 & \alpha_2 & 0 & 0 \\ 0 & 0 & 0 & \alpha_2 & 0 \\ 0 & 0 & 0 & 0 & \alpha_3 \end{bmatrix}$$

The tuning parameters are tuggled by an optimisation procedure described in the next section, so as to save development time.

4) Adaptive observer: This speed observer is based on the Lyapunov theory and is well described in [11], [12]. The design of this observer is composed of two successive steps :

- The first one consists in the design of a full order flux observer as a Luenberger or stochastic one. At this step, the rotor speed is supposed to be known. We opt for a sub-optimal Kalman filter which is equivalent to a Luenberger observer.
- The second step consists in the design of the speed estimator composed of a PI controller. The output of the adaptive mechanism is the rotor speed which is used at the next sample time in the flux observer. Figure (2) represents the adaptive observer structure.

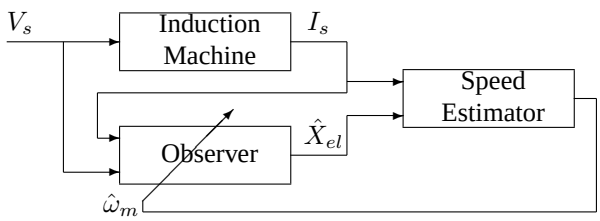

Fig. 2. Adaptive Observer diagram

The flux observer is based on the discrete state space model described in equation (II-B.2). The sub-optimal Kalman filter uses the matrix gain $K[+\infty]$ defined as $\lim_{k\to+\infty} K[k]$ to reduce the number of operations. The Kalman gains represented in Fig. (3) depend only on the mechanical speed.

$$K^t = \begin{bmatrix} K_{11} & 0 & K_{13} & K_{14} \\ 0 & K_{11} & -K_{14} & K_{13} \end{bmatrix}$$

The symmetries, anti-symmetries and zeros present in these structures reduce the computational cost of the Kalman filter, since they reduce the number of distinct values [22], which can be computed by the following rational function :

$$K_{ij}(\omega_m) = \frac{\sum_{k=0}^{N} b_{k,ij}\,\omega_m^k}{1 + \sum_{k=1}^{M} a_{k,ij}\,\omega_m^k}$$

where N and M are two integers different for each gain.

The speed estimator is based on the Lyapunov function $V = e^t e + \frac{(\hat{\omega}_m - \omega_m)^2}{\lambda}$ with $\lambda > 0$ and $e^t = [i_{s\alpha} - \hat{i}_{s\alpha},\, i_{s\beta} - \hat{i}_{s\beta},\, 0,\, 0]$ (we suppose that $\phi_{r\alpha} = \hat{\phi}_{r\alpha}$ and $\phi_{r\beta} = \hat{\phi}_{r\beta}$), which yields the speed estimator :

$$\frac{d}{dt}\hat{\omega}_m = K_i\,(e_{is\alpha}\hat{\Phi}_{r\beta} - e_{is\beta}\hat{\Phi}_{r\alpha})$$

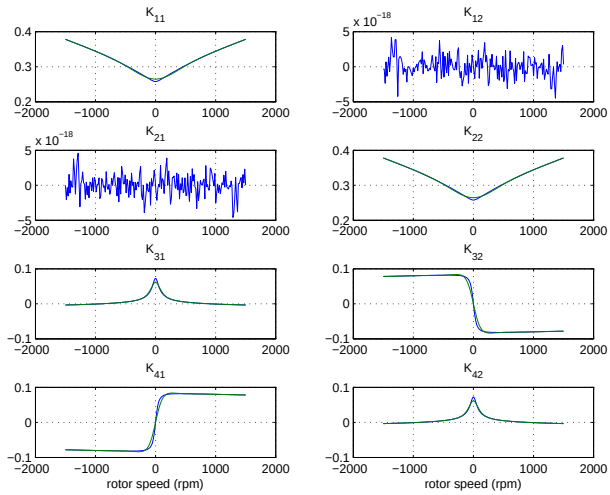

Fig. 3. Kalman filter gains as function of the rotor speed.

where K_i is strictly positif. To improve the speed estimation during transient, a proportional term K_p is added :

$$\begin{aligned}\hat{\omega}_m[k] &= K_p\left(e_{is\alpha}\hat{\Phi}_{r\beta} - e_{is\beta}\hat{\Phi}_{r\alpha}\right)\\ &+ K_i\int_0^{k\,T_e}\left(e_{is\alpha}\hat{\Phi}_{r\beta} - e_{is\beta}\hat{\Phi}_{r\alpha}\right)dt\end{aligned}$$

As the EKF, the tuning parameters are set by the optimisation procedure.

To increase the reliability of the control strategy, the control decision block must be able to give to the controller the most accurate information on the mechanical speed. To achieve this goal a comparison is made between the output of the sensor and those of the observers and a voting algorithm decides on line which information will be introduced in the controller. The strategy is described in the following diagram 4.

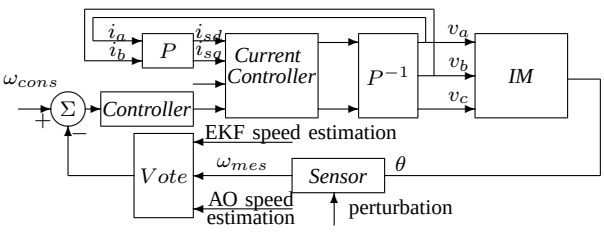

Fig. 4. Fault tolerant controller structure.

III. Observer tuning

A. Experimental system

Experimental tests have been carried out using the three-phase $1.2k$W induction motor with the parameters given in Table II. The proposed controller and observers are implemented on a dSPACE DS1104 platform using a sampling time of 125μs. The control voltages applied to the stator are obtained from a three-phase PWM inverter fed by a 300V DC source. The controller is a classical Field Oriented Control composed of four IP regulators (two current regulators in the (d,q) reference frame, one flux regulator and one speed regulator).

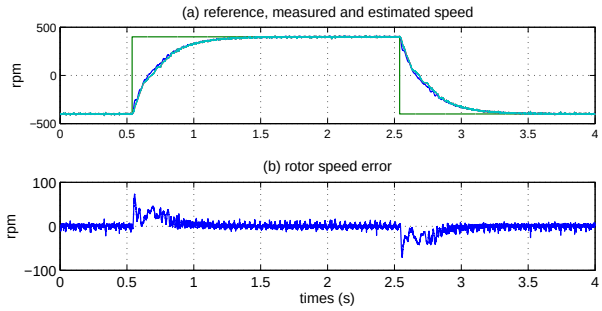

Fig. 5. Experiment result without closed loop speed estimation.

B. Tuning

To find relevant values of the parameters α_1, α_2 and α_3 for the EKF and K_p, K_i for the adaptive observer, we have minimized the mean square error of the mechanical speed under some given experimental conditions shown in figure 5. The data are collected from a simulated AC motor whose speed controller uses the real values of the rotor flux. The EKF and adaptive observer are not included in the closed loop. This minimization process finds the values of the freedom degree which yields the best estimated speed in a nominal case (no parameter variation). This approach provides less computational time compared to an optimization procedure where the observers are included in the closed loop.

The optimum parameters for this test bench are :

- EKF : $\alpha_1 = 9.83.10^{-4}$, $\alpha_2 = 9.32.10^{-12}$, $\alpha_3 = 1.20.10^{1}$
- AO : $K_p = 0.404$, $K_i = 179.8$

Fig. 5 shows an experimental result where the EKF is now included in the speed regulation loop. No instability phenomena are oberved during experimental tests with the sensorless speed control. This proves the validity of the open loop parameters tuning approach.

The next step is to determine for each observer the reliability coefficients required by the voting algorithm of the fault tolerant controller described in the next section. Therefore, extensive simulations and off-line experimental tests have been carried out and the 2 observers are compared in function of :

- speed level,
- robustness to stator resistance variation.

Fig. (6) represents a typical open-loop simulation because the estimated speed and flux are not included in the controller. In conclusion of these extensive simulations, we can notice that :

- the EKF has better performances on the whole speed range compared to the AO,
- the AO is less sensitive to stator resistance variation at high speed.

IV. Fault tolerant controller

The control decision block relies on an approval voting algorithm type in which the emerging output has the highest approval. The weighted averaged voters [23] suffers

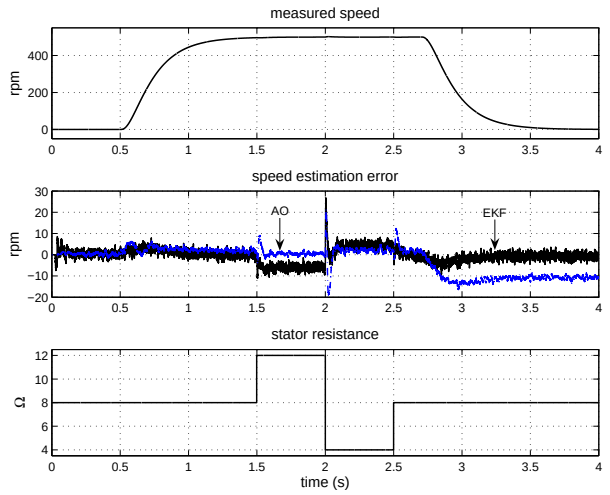

Fig. 6. Estimated Speed by the EKF (solid line) and adaptive observer (dashed line), with stator resistance variation.

from a lack of accuracy because in normal operating conditions, i.e. without a fault sensor, the emerging output is a combination of the three inputs. The other method which is used here is the Maximum Likelihood voting algorithm [24] in which a probability for each input is computed based on reliability coefficients. The computation of the probability coefficients is slightly modified to introduce a threshold and in normal operating conditions to choose the speed sensor as the emerging output.

$$\Delta_k(i) = \begin{cases} f_k & \text{if } |x_i - x_k| \leq Dmax_{ik} \\ \frac{1-f_k}{N-1} & \text{else} \end{cases}$$

After simulations and off-line experimental simulations, the threshold $Dmax_{ik}$ is set to 20 rpm at zero speed and to 10 rpm at the nominal speed. The reliability coefficients determined over the whole speed range for each observer based on the experimental measurements are:

- for EKF : the reliability coefficient is set to 0.95 on the whole speed range.
- AO : the reliability coefficient change from 0.90 at zero speed to 0.95 at the nominal speed. Therefore the two observers are complementary.
- Speed sensor : the reliability coefficient is constant (0.99) on the entire speed range.

To evaluate the fault tolerant controller, a speed sensor failure and recovery is introduced between 1 and 1.5s and also between 2 and 3s for two different operating points, 500 and 1000 rpm. The speed estimation error is evaluated as the difference between the real speed (non erroneous measured speed) and the emerging output of the voting algorithm. Fig. 7, 8 and 9 show the response of the fault tolerant controller where the voting algorithm output is used in the FOC. At low and medium speed, the EKF output is selected in the case of failure. At high speed, it is the AO output which is engaged to maintain the level of performance. As it is stated in paragraph 3, the AO seems to be less sensitive to the stator resistance variation

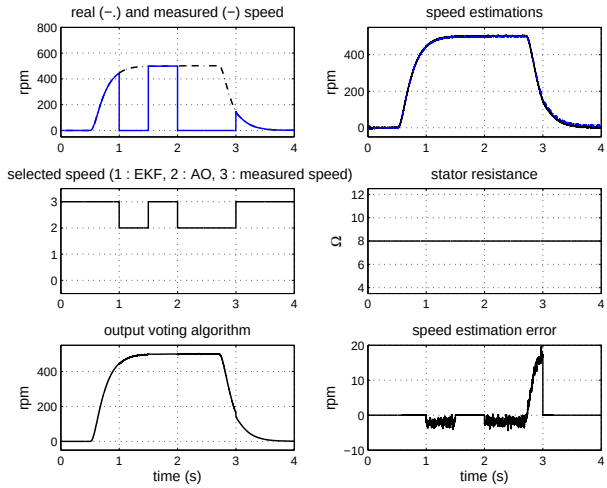

Fig. 7. In line test of the voting algorithm at medium speed.

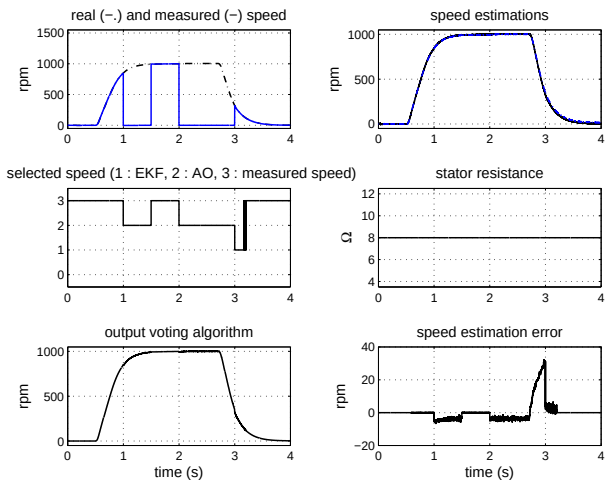

Fig. 8. In line test of the voting algorithm at high speed.

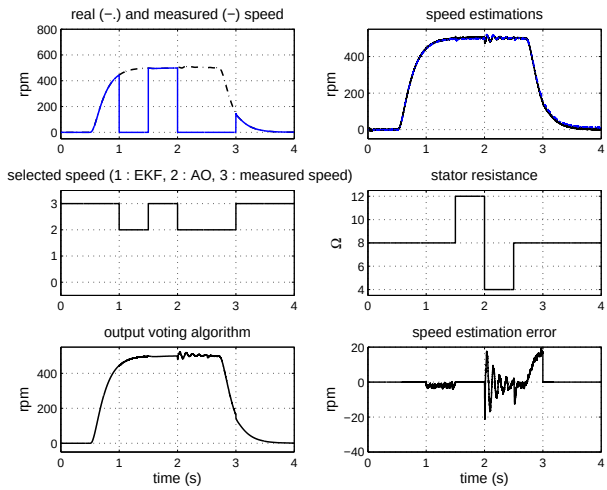

Fig. 9. In line test of the voting algorithm at medium speed with stator resistance variation.

compared to the EKF. Fig. 9 confirms the robustness of the AO output. The transition between the sensor output and the observers' is smooth, the level of performance is maintained and the system is also robust to stator resistance variation.

V. Conclusion

In this paper we have described a fault tolerant controller for an induction motor drive well suited in sensitive applications such as Electric Vehicle (EV) or Hybrid Electrical Vehicle (HEV). The controller is based on a Fiel Oriented Control with 4 IP regulators and a speed sensor to guarantee the best dynamic performances required by the application. To maintain a good level of performance and to increase the reliability in the event of sensor loss or sensor recovery, a sensorless controller based on an Extended Kalman Filter (EKF) and an Adaptive Observer (AO) has been designed.The tuning of the observers has been developed based on extensive simulations, experimental results and an optimization procedure within an open-loop type approach. Experimental results of the EKF used in closed loop prove the validity of the tuning. The control system reorganization is based on a control decision block which has to select the most appropriate speed information for the speed regulator depending on the electric propulsion operating conditions. A Maximum Likelihood voting algorithm is used to determine the emerging output among the sensor and the observers. The voting algorithm principle relies upon reliability coefficients setting. Extensive study allows to set those coefficients on the entire speed range and a complementarity is found between the two observers. The results of the control system show the effectiveness of the approach. The transition between the sensor output and the observers' is smooth, the level of performance is maintained and the system is also robust to stator resistance variation.

References

[1] M. Zeraoulia, M.E.H. Benbouzid and D. Diallo, "Electric motor drive selection issues for HEV propulsion systems: A comparative study," *IEEE Trans. Vehicular Technology*, 2006.

[2] Y.S. Jeong, S.K. Sul, S.E. Schulz and N.R. Patel, "Fault detection and fault-tolerant control of interior permanent-magnet motor drive system for electric vehicle," *IEEE Trans. Industry Applications*, vol. 41, n1, pp. 46-51, January-February 2005.

[3] D. Diallo, M.E.H. Benbouzid and A. Makouf, "A fault-tolerant control architecture for induction motor drives in automotive applications," *IEEE Trans. Vehicular Technology*, vol. 53, n6, pp. 1847-1855, November 2004.

[4] M.B. de Rossier Corra, C.B. Jacobina, E.R.C. da Silva and A.N. Lima, "An induction motor drive system with improved fault tolerance," *IEEE Trans. Industry Applications*, vol. 37, n5, pp. 873-879, May-June 2001.

[5] M. Hilairet, F. Auger, "Frequency estimation for sensorless control of induction motors," *IEEE ICASSP 2001*, Salt Lake City, Utah (US), May 2001.

[6] T. Du, P. Vas, A.F. Stronach, "Application of non-linear estimators in speed-sensorless high-performance induction motor drives," *Proc ICEM'94*, pp 403-408, Paris, 1994.

[7] I. Zein, "Application du filtre de Kalman et de l'observateur de Luenberger à la commande et à la surveillance de la machine asynchrone," *PhD. Thesis from l'Université de Technologie de Compiègne (UTC), France*, Sep. 2000.

[8] D. Atkinson, P. Acarnley, J. Finch, " Observers for Induction motor state and parameter estimation," *IEEE Transactions on Industry Applications*, Vol 27, No 6, pp 1119-1127, Nov./Dec. 1991.

[9] E.G.V. Westerholt, M. Pietrzak-David, B. de Fornel, "Extended state estimation of nonlinear modeled induction machines," *Power Electronics Specialists Conference, PESC'92*, Vol 1, pp 271-278, 1992.

[10] El Hassan, "Commande haute performance d'un moteur asynchrone sans capteur de vitesse par contrle direct du couple," *PhD. Thesis from INPT Toulouse, France*, 1999.

[11] H. Kubota, K. Matsuse, T. Nakano, "DSP-based speed adaptive flux observer of induction motor," *IEEE Transactions on Industry Applications*, Vol 29, No 2, pp 152-156, Mars/Avril 1993.

[12] M. A. Purwoadi, "Réglage non-linéaire du variateur de vitesse asynchrone sans capteur mécanque,contribution à la commande par linéarisation exacte entrées-sortie et à l'observation du flux rotorique," *PhD. Thesis from INPT Toulouse, France*, N1165, 1996.

[13] Y.N. Lin, C.L. Chen, "Adaptive pseudoreduced-order flux observer for speed sensorless field-oriented control of IM," *IEEE Transactions on Industrial Electronics*, Vol. 46, No. 5, pp 1042-1045, Octobre 1999.

[14] M. Bodson, J. Chiasson, "Comparison of sensorless speed estimation methods for induction motor control," *Proceedings of the American Control Conference*, mai, 2002.

[15] S. Siala et F. Terrien, "Robust sensorless induction motor control for electric propulsion ship," *EPE 2003*, Toulouse, Septembre 2003.

[16] S.R. Bowes, A. Sevinc, D. Holliday, "New natural observer applied to speed-sensorless DC servo and induction motors," *IEEE Transactions on Industrial Electronics*,Vol 51, N5, pp 1025-32, Oct. 2004.

[17] R. Marino, P. tomei, C.M. Verrelli, "A global tracking control for speed-sensorless induction motors," *Automatica*, Vol. 40, pp 1071–1077, 2004.

[18] M.S. Santina, A.R. Stubberud, G.H. Hostetter, "Discrete-time equivalents to continuous-time systems," *The control Handbook*, IEEE Press, 1996.

[19] C. Attaianese, V.N. Perfetto, G. Tomasso, "Vectorial torque control : a novel approach to torque and flux control of induction motor drives," *IEEE Transactions on Industry Applications*, Vol 35, No 6, pp 1399-1405, Nov./Dec. 1999.

[20] M.S. Grewal, A.P. Andrews, "Kalman filtering, theory and practice," *Prentice Hall*, Englewood Cliffs, New Jersey, 1993.

[21] M. Hilairet, E. Berthelot "Application du filtrage de Kalman double niveaux à l'estimation de la vitesse mécanique d'une machine asynchrone" *Conférence Internationale Francophone d'Automatique (CIFA)*, Bordeaux, May 2006.

[22] M. Hilairet, F. Auger, C. Darengosse, "Two efficient Kalman filters for flux and velocity estimation of induction motors," *Proc IEEE PESC'00*, Vol 2, pp 891-896, juin 2000.

[23] Latif-Shabgahi, G. Bass, J.M. Bennett, S. "History-based weighted average voter: a novel software voting algorithm for fault-tolerant computer systems", *Parallel and Distributed Processing, 2001. Proceedings. Ninth Euromicro Workshop on* page(s): 402-409.

[24] Y. Leung, "Maximum Likelihood Voting for Fault Tolerant Software with Finite Output Space", *IEEE Trans. Reliability*, vol. 14, n3, pp. 419 - 427, Sept. 1995 .

TABLE II

Induction machine parameters

Rated Flux	$\Phi_r = 1.07\ Wb$
Rated Power	$P_n = 1.2\ kW$
Rated Torque	$C_n = 7\ Nm$
Rated Speed	$N = 146.6\ rad/s$
Rated Voltage	$V_n = 200\ V$
Rated Current	$I_n = 4,50\ A$
Stator resistance	$R_s = 8\ \Omega$
Rotor resistance	$R_r = 4\ \Omega$
Stator inductance	$L_s = 0,47\ mH$
Rotor inductance	$L_r = 0,42\ mH$
Mutual inductance	$M_{sr} = 0,42\ mH$
Number of poles	$2p = 4$
Inertia	$J = 0,06\ Kg\,m^2$
Friction coefficient	$f = 0,04\ Nm/s$